Worst-Case Adaptive Model of Field Penetration into Shielding Enclosure

Eugene Sinkevich
EMC R&D Laboratory
Belarusian State University
of Informatics and Radioelectronics
Minsk, Belarus
esinkevich@bsuir.by

Yauheni Arlou
EMC R&D Laboratory
Belarusian State University
of Informatics and Radioelectronics
Minsk, Belarus
emc@bsuir.by

Natalia Sinyak
EMC R&D Laboratory
Belarusian State University
of Informatics and Radioelectronics
Minsk, Belarus
emc@bsuir.by

Ivan Shakinka
EMC R&D Laboratory
Belarusian State University
of Informatics and Radioelectronics
Minsk, Belarus
emc@bsuir.by

Xie Ma
China Electronics Technology
Cyber Security Co., Ltd.,
Chengdu, Taiyuan, China
18081045600@163.com

Wen-Qing Guo
China Electronics Technology
Cyber Security Co., Ltd.
Chengdu, Taiyuan, China
gigigigogogo@126.com

***Abstract*—A new approach to the description of the resonance properties of objects (vehicle compartments, cases of electronic equipment, connecting cables, etc.) in the problems of the analysis of electromagnetic compatibility and electromagnetic protection is proposed. The essence of the approach is to create worst-case adaptive models that adjust (adapt) a priori unknown resonance frequencies of the simulated objects for each input stimulus in such a way as to provide the worst value of the criterion of electromagnetic compatibility (or protection criterion). Within the framework of the proposed approach, a worst-case adaptive model of the penetration of electric and magnetic fields into a shielding enclosure (e.g., into a vehicle compartment) is developed; the model is based on the existing non-adaptive model using analytical expressions for the field inside a rectangular waveguide. The developed model is validated by the following example: the impact of external electromagnetic pulses (the radar pulse and E1 HEMP) on a vehicle (jeep) is analyzed; the results of the calculation by the developed model are compared with the results of the FDTD calculation.**

Keywords—electromagnetic interference, electromagnetic shielding, EMP radiation effects, time-domain analysis

I. Introduction

The wave dimensions of objects increase with increasing the frequency of electromagnetic disturbance. As a result of this, resonances are observed in many objects (compartments of vehicles, cases of electronic equipment, connecting cables, etc.). That is why the amplitude-frequency characteristics (AFCs) of such objects at high frequencies consist of many peaks observed at resonant frequencies and dips between these peaks [1], [2], [3].

When modeling parasitic electromagnetic couplings through such objects, the resonant frequencies are usually difficult to predict for the following reason: small errors and (or) simplifications in the mathematical description of object properties (geometry, structure) can lead to significant changes in the calculation results and to their deviation from the results of measurements [4], [5]. Incorrect prediction of the resonant frequencies by particular-case models (for example, by models of computational electromagnetics) can lead to erroneous prediction of absence of interference if the receptor or input disturbance is narrow-band (namely, if the bandwidth of the disturbance or the receptor is less than the frequency difference between two adjacent resonances of the object).

In order to avoid the erroneous prediction of absence of interference, frequency-domain worst-case envelope models are widely used for the analysis and design of electromagnetic compatibility (EMC) and electromagnetic protection. These models are formulated according to the following principle: it is conventionally considered that the resonance in the simulated object is observed at each frequency in the high-frequency region, therefore the worst-case model of AFC of the object is the upper envelope of the peaks mentioned above. The worst-case envelope model of AFC can be synthesized by the following methods: 1) analytically [6, p.227], [7], [8], [9]; 2) statistically, i.e., by processing the Monte Carlo simulation results [10], [4] or measurement results; 3) heuristically (for example, by connecting the maximums of one particular case of AFC with straight-line segments) [11], [12].

However, the worst-case envelope models are inapplicable in a situation where the input disturbance and the receptor are broadband: if the bandwidth of both the disturbance and the receptor is K times the peak width of the AFC of the object, then the use of the worst-case envelope model leads to an excessive overestimation of the response energy (or power for periodic disturbances) dissipated in the susceptible element of the receptor [13] approximately by a factor of K; the value of K may be so large that the worst-case envelope model is inadequate (useless in practice).

The purpose of this work is to develop a method for modeling an object whose resonant frequencies are a priori unknown; the method must make it possible to obtain adequate worst-case estimations of the critical parameters (energy, power, amplitude of time-domain realization) of the object response to an arbitrary electromagnetic disturbance in case of an arbitrary receptor bandwidth.

II. Adaptation of Resonant Frequencies of Simulated Object to Input Disturbance

The most obvious way to achieve the formulated purpose is to combine the particular-case model and the worst-case envelope model. This can be done, for example, by the following algorithm: 1) estimate the frequency bandwidth of the input disturbance, the width of a peak in the AFC of the modeled object, and the bandwidth of the receptor; 2) based on these three values, decide whether to use the particular-case model or the worst-case envelope model. The limitation of such way is the high complexity of developing the

DOI: 10.1109/EMCEurope51680.2022.9901273

decision rules due to the need of analyzing a large number of specific cases.

In this paper, a more reliable and physically understandable approach is proposed: to use a particular-case model in which to change (adapt) a priori unknown resonant frequencies of the object automatically in a way that provides the worst value of the EMC criterion (or electromagnetic protection criterion) for a given input disturbance. Since such a model adapts the resonance frequencies of the object to the input disturbance according to the worst-case criterion, it is called the worst-case adaptive model.

In order to do the adaptation, it is necessary to 1) implement the possibility of synchronous change of resonance frequencies for the particular-case model using some control parameter (for example, the phase of the reflection factor, see Section III.B) and 2) perform optimization, i.e., search for the worst value of the EMC criterion, in the area of definition of the control parameter.

In the general case, the optimization should be carried out numerically, but this leads to an increase of the simulation time by a large factor. Therefore, in this paper, we propose a simplified algorithm of semi-analytical optimization: 1) by using the worst-case envelope model, calculate the response spectrum $S_{R,wc}(f)$ at the input of the susceptible element of the receptor [13]; 2) find the frequency f_{mx} at which the modulus $|S_{R,wc}(f)|$ of the calculated spectrum is maximum; 3) change the value of the control parameter so that the nearest resonant frequency of the simulated object coincides with f_{mx}. In most situations, this algorithm makes it possible to maximize the response energy (or power) dissipated in the susceptible element of the receptor.

III. Example of Application of Proposed Approach: Model of Shielding by Conductive Enclosure

A. Worst-Case Envelope Model

This section contains a brief description of the worst-case envelope model developed earlier in [9].

A shielding enclosure is approximated by a rectangular parallelepiped with apertures in walls, as shown in Fig. 1.

The shielding effectiveness S_E (S_H) is defined as

$$S_E = 20\lg(|E_0|/|E'|), \quad S_H = 20\lg(|H_0|/|H'|), \qquad (1)$$

where $|E'|$ is the electric field amplitude in the shielded zone; $|E_0|$ is the incident electric field amplitude; $|H'|$ and $|H_0|$ are the corresponding amplitudes of the magnetic fields.

The incident electromagnetic wave is perpendicular to the wall of the shielding enclosure with apertures.

A rectangular waveguide of dimension $L_x \times L_y$ is assigned to the shielding enclosure. The waveguide cutoff frequency, i.e., the frequency of fundamental mode TE(1,0), is $f_c = c/(2\max(L_x, L_y))$. The propagation constant γ and the characteristic impedance Z for a lossless waveguide are:

$$\gamma = \frac{2\pi f}{c}\sqrt{1-(f_c/f)^2}, \quad Z = Z_0\Big/\sqrt{1-(f_c/f)^2}, \qquad (2)$$

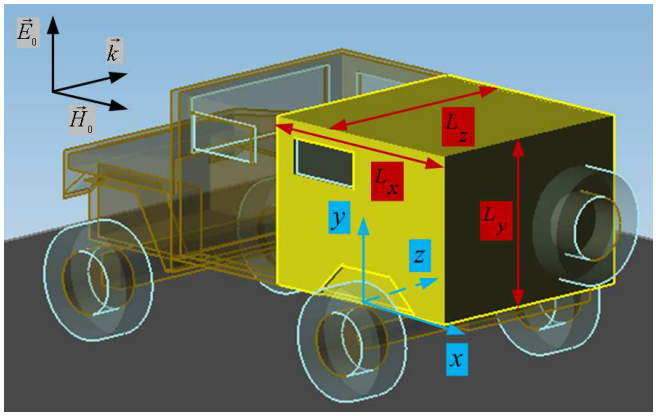

Fig. 1. Geometry of shielding enclosure with apertures in walls. L_x, L_y, L_z are dimensions of enclosure, k is wave vector

where $Z_0 = 120\pi$ is characteristic impedance of free space.

The worst-case envelope model is defined in [9] as a sum of a reverberation component and line-of-sight fields. The reverberation component represents the electric and magnetic fields arising due to multiple reflections from the walls inside the enclosure.

The radiation penetrates through the illuminated wall, and multiple reflections from the back and front walls arise inside the enclosure. Herein and below, the quantities noted by index f correspond to the front wall, and the quantities noted by index b correspond to the back wall. Intrinsic Q-factor of an empty metallic enclosure is $Q_0 = 2\pi P_{st}/P_{out} = 2\pi \cdot 10^{0.5(S_{Gf}+S_{Gb})/10}$, where S_{Gf} (S_{Gb}) is the shielding effectiveness of the front (back) wall.

The simplified particular-case model of the field distribution inside the enclosure is as follows [9]:

$$\begin{aligned}
E_{y10} &= -j|E'|\left[e^{-j\gamma' z} + R_b e^{-j\gamma'(2L_z - z)}\right]G(f)\cos(\pi x/L_x),\\
H_{x10} &= j|H'|\left[e^{-j\gamma' z} - R_b e^{-j\gamma'(2L_z - z)}\right]G(f)\cos(\pi x/L_x),\\
H_{z10} &= |H'|\left[e^{-j\gamma' z} - R_b e^{-j\gamma'(2L_z - z)}\right]G(f)\sin(\pi x/L_x),\\
G(f) &= (1 - R_f R_b \exp(-j\gamma' 2L_z))^{-1},
\end{aligned} \qquad (3)$$

where $j = \sqrt{-1}$ is imaginary unit; $|E'|$ and $|H'|$ are the wave amplitudes calculated according to (1) and determined by the averaged power penetrating through the illuminated wall; γ' is the propagation constant:

$$\begin{aligned}
&\gamma' = \gamma A(Q), \quad Z' = Z A(Q), \quad A(Q) = 1 + \xi(Q) - j\xi(Q),\\
&\xi(Q) = \sqrt{1 - \left(4\pi/\ln(1 - 2\pi/Q)\right)^2},
\end{aligned} \qquad (4)$$

where γ and Z are defined by (2); $A(Q)$ is the parameter describing the attenuation; R_f and R_b are the reflection coefficients of the front and back wall, respectively.

The maxima of the term $G(f)$ in (3) are observed in the high-frequency band at resonance frequencies $f_1(m)$, where m is the resonance number [9]. In order to obtain the worst-case envelope model, these maxima are connected by straight lines as follows:

$$G_{hf}(f)=\begin{cases}\left|G(f_1(1))\right|, & f\in(f_c,f_1(1)),\\ \left|u\,f+v\right|, & f\in[f_1(1),\infty),\end{cases}$$
$$u=\Delta G/\Delta f_1,$$
$$v=[G(f_1(m))f_1(m+1)-G(f_1(m+1))f_1(m)]/\Delta f_1, \quad (5)$$
$$\Delta G=G(f_1(m+1))-G(f_1(m)),$$
$$\Delta f_1=(f_1(m+1)-f_1(m)).$$

The worst-case envelope model for the high-frequencies

$$E_{hf}(f)=4\left|E_0\right|10^{-S_E/20}G_{hf}(f),$$
$$H_{hf}(f)=4\left|H_0\right|10^{-S_H/20}G_{hf}(f) \quad (6)$$

is obtained by replacing the term $G(f)$ in (3) by $G_{hf}(f)$.

A transition model is defined as a weighted average of the low-frequency and high-frequency models:

$$E_{con}(f)=E_{lf}(l_1f_c)\left(1-F_{tr}(f)\right)+E_{hf}(l_2f_c)F_{tr}(f),$$
$$H_{con}(f)=H_{lf}(l_1f_c)\left(1-F_{tr}(f)\right)+H_{hf}(l_2f_c)F_{tr}(f), \quad (7)$$

where $E_{lf}(f)$ and $H_{lf}(f)$ is the low-frequency model given by (3); $F_{tr}(f)$ is the weighting function:

$$F_{tr}(f)=3\left(\chi(f)\right)^2-2\left(\chi(f)\right)^3,$$
$$\chi(f)=(f/f_c-0.9)/(1.1-0.9). \quad (8)$$

The wideband worst-case envelope model for the reverberation component of electric field $E_{REV\,wce}$ and magnetic field $H_{REV\,wce}$ is defined as follows:

$$E\{H\}_{REV\,wce}(f)=\begin{cases}E\{H\}_{lf}(f), & f\in(0,0.9f_c),\\ E\{H\}_{\text{con}}(f), & f\in[0.9f_c,1.1f_c],\\ E\{H\}_{hf}(f), & f\in(1.1f_c,\infty),\end{cases} \quad (9)$$

where notation $E\{H\}$ means the choice of E or H.

The model can be expressed in the form of AFC by finding a ratio of (9) to the incident field amplitude:

$$AFC_{E\{H\}REV\,wce}(f)=|E\{H\}_{REV\,wce}(f)|/|E\{H\}_0|. \quad (10)$$

B. Worst-Case Adaptive Model

The resonant frequencies in particular-case model (3) are adapted to a given disturbance by the following algorithm:

1. Compute the worst-case envelope AFC $AFC_{E\{H\}wce}$ of the spurious coupling "external field – internal field" as a sum of the reverberation component AFC (10) and the line-of-sight component AFC [9].

2. Compute the phase-frequency characteristic (PFC) $PFC_{E\{H\}wce}$ of the spurious coupling by the Minimum Phase Algorithm [14].

3. Calculate the worst-case envelope model of the transfer function of the spurious coupling: $T_{E\{H\}wce}(f)=AFC_{E\{H\}wce}e^{jPFC_{E\{H\}wce}}$.

4. Compute the transfer function $T_{E\{H\}path}$ of the influence path containing the spurious coupling. Note: besides this coupling, the influence path can include filters and other spurious couplings, e.g., "internal field – wire".

5. Compute the complex spectrum of the response at the receptor: $S_{wce}(f)=E\{H\}_0(f)\cdot T_{E\{H\}path}$, where $E\{H\}_0(f)$ is the spectrum of the input disturbance (i.e., the incident field).

6. Find a frequency f_{mx} at which the maximum of the amplitude spectrum $|S_{wce}(f)|$ of the response occurs.

7. If $f_{mx}<f_{CH}$, then set $f_{mx}=f_{CH}$, because a resonance cannot arise in below-cutoff waveguide. Here $f_{CH}=1.1f_c$ is the upper frequency of connection between the low-frequency and high-frequency models in (9).

8. Obtain the worst-case adaptive model of the AFC $AFC_{E\{H\}REV\,wca}(f)$ for the reverberation component of the internal field:

8.1. Move the nearest resonant frequency described by the term $G(f)$ in (3) to the frequency f_{mx}. To do this, change the phase of the reflection factor R_f in such a way that the phase of expression $R_f{}^{\text{mod}}R_be^{-j\gamma'2L_z}$ contained in (3) is equal to zero at the frequency f_{mx}. Here, $R_f{}^{\text{mod}}$ is the modified value of R_f:

$$R_f{}^{\text{mod}}(f)=R_f(f)\cdot e^{-j\arg\left[R_f(f_{mx})R_b(f_{mx})\exp(-j\gamma'(f_{mx})2L_z)\right]}. \quad (11)$$

8.2. Calculate the desired AFC $AFC_{E\{H\}REV\,wca}(f)$ by (10) with the following peculiarities: a) use the resonant-peak term $G(f)$ defined in (3) instead of the envelope $G_{hf}(f)$ defined by (5) and b) use the reflection factor $R_f{}^{\text{mod}}$ instead of R_f in (3). Note: as a result, one of peaks of the calculated AFC is observed at the frequency f_{mx}.

9. Given the $AFC_{E\{H\}REV\,wca}(f)$, calculate the worst-case adaptive model $T_{E\{H\}wca}(f)$ of the transfer function of the spurious coupling (similarly to items 1, 2 and 3).

10. Recalculate the spectrum of the response at the receptor by replacing the transfer function $T_{E\{H\}wce}(f)$ of the worst-case envelope model (see item 3) with the transfer function $T_{E\{H\}wca}(f)$ of the worst-case adaptive model:

$$S_{wca}(f)=S_{wce}(f)\cdot T_{E\{H\}wca}(f)/T_{E\{H\}wce}(f). \quad (12)$$

11. Compute the response waveform $S_{wca}(t)$ as the inverse FFT of the spectrum (12).

The obtained model adapts the AFC of the influence path to a given disturbance in order to ensure the worst-case

nature of the response assessment. The adaptation is performed by changing the AFC of the model for the reverberation component of the internal field.

To illustrate the adaptation principle, the AFCs of the reverberation component of the field inside a vehicle compartment are calculated by using the considered models. The AFC of the particular-case model (black line in Fig. 2) is nonuniform due to resonances. The AFC of the worst-case envelope model bypasses the AFC of the particular-case model with margin. One of the peaks of the worst-case adaptive model is located at the frequency f_{mx} (74.6 MHz in this case). The peaks of the worst-case adaptive model exceed the peaks of the particular-case model because the adaptive model uses the same worst-case approximations as the worst-case envelope model: 1) the field amplitude at resonance frequencies is the same throughout the compartment and is maximal, 2) the multiplier $e^{-j\gamma' z} + R_b e^{-j\gamma'(2L_z - z)}$ in (3) has the worst value of 2.

C. Validation of Worst-Case Adaptive Model

As an example of application of the worst-case adaptive model, the influence of E1 HEMP electromagnetic pulse and a radar pulse on a vehicle is analyzed. The E1 HEMP pulse is wideband, the radar pulse is narrowband.

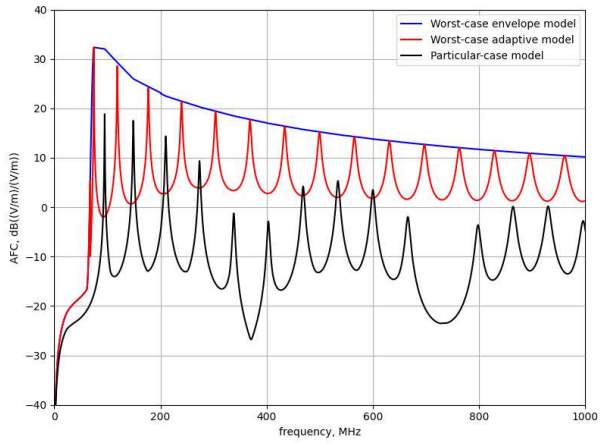

Fig. 2. AFC for model of reverberation component of field in observation point located inside the compartment "back" (see Fig. 3)

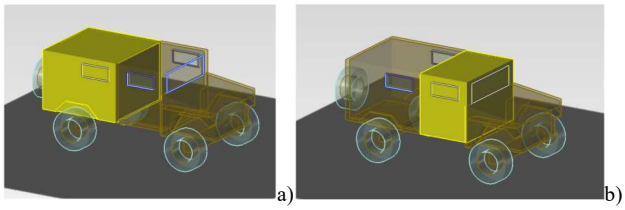

Fig. 3. Analyzed compartments of the vehicle: (a) "back", (b) "front"

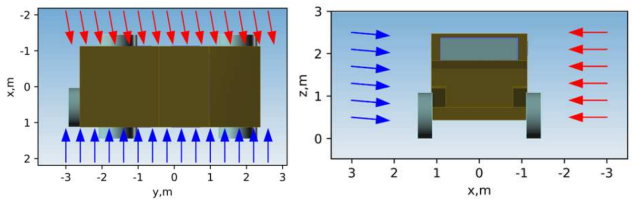

Fig. 4. Directions of incidence of electromagnetic disturbances: E1 HEMP pulse (blue arrows) and radar pulse (red arrows)

The simplified geometric model of the vehicle is used for computer simulations (see Fig. 1). Two compartments are specified in the vehicle: "back" and "front" (see Fig. 3). The directions of propagation of the pulses are shown in Fig. 4. The coordinate system in this Subsection (see Fig. 4) differs from the coordinate system of the shielding model (see Fig. 1), therefore coordinate transformations are applied.

The E1 HEMP pulse is described by the double exponential model. The rise time of the pulse is 2.5 ns and the pulse duration is 23 ns. The amplitude of the incident pulse is taken equal to 1 kV/m (see the green line in Fig. 6), this corresponds to the distance of about 800 km from the disturbance source to the vehicle.

The radar pulse is described by the trapezoidal model. The pulse duration is 2 μs and the rise time is 20 ns (1% of the pulse duration). The amplitude of the incident pulse is taken equal to 100 V/m (see the green line in Fig. 8), this corresponds to the distance of about 500 m from the radar to the vehicle. The carrier frequency of the pulse is chosen to be 154.8 MHz, which is equal to one of the resonant frequencies of the "back" compartment (see Fig. 3).

The duration of the simulation interval is chosen equal to *Tmax* = 5 μs. This duration does not change the waveforms of the responses in observation points, since the field level inside the vehicle decreases to almost zero by the end of the simulation interval (see Figs. 6 and 8).

The number of time-domain samples is chosen equal to 32 768 for simulations using the worst-case (envelope and adaptive) models. Since *Tmax* = 5 μs, the time step is 152.6 ps, the frequency step is 200 kHz, and the maximum frequency of the simulation is 3.28 GHz.

The maximum frequency of simulations using the FDTD method is chosen equal to 600 MHz for the following reasons. Firstly, the frequency range of simulation must contain the main part of the energy of the E1 HEMP pulse (the range from 1.6 kHz to 26.8 MHz contains 90% of the energy of this pulse). Secondly, the maximum frequency of simulation must be greater than the carrier frequency of the radar pulse. Thirdly, the computational resources required for FDTD simulation increase rapidly with increasing the maximum frequency of simulation.

The spatial distribution of field levels obtained by FDTD method is highly nonuniform: field minima and maxima arising due to resonances and wave propagation effects are observed. Due to this nonuniformity, the direct comparison of the simulation results obtained by using the worst-case models (which describe only the maxima of the field) with the results obtained by FDTD method is not correct. Therefore, the results computed by the worst-case (envelope and adaptive) models are compared with the results obtained by using a spatial-domain worst-case FDTD model. This worst-case FDTD model is obtained heuristically as follows: after performing the FDTD simulation, the worst point (i.e., the point with the maximum field level) is found in the vicinity of the observation point and analyzed. The vicinity is defined as the intersection of two volumes: 1) a cube with the edge length *d* and 2) the inside volume of the compartment to which the observation point belongs (Fig. 5). When considering the wideband pulse, the edge length *d* is taken equal to a wavelength corresponding to the minimal resonant frequency of the compartment. If the observation point belongs to compartment "back", the cube edge length *d* is

equal to 3.15 m (this corresponds to the resonant frequency of 95 MHz). If the observation point belongs to compartment "front", then d is equal to 2.63 m (this corresponds to the resonant frequency of 114 MHz). When considering the narrowband pulse, the length d of the cube edge is taken equal to the wavelength corresponding to the carrier frequency of the pulse (i.e., $d = 1.93$ m).

During the simulation, 2000 observation points are analyzed: 1000 points in each compartment of the vehicle. The observation points are located inside each compartment on an uniform spatial grid of 10x10x10 points. In the "back" compartment, the distances between adjacent points along the x, y, z axes are equal to 0.205 m, 0.221 m, and 0.157 m, respectively. In the "front" compartment, these distances are 0.205 m, 0.133 m, and 0.157 m.

The simulation is performed on a personal computer with 16 GB of RAM and an "AMD Ryzen™ 5 3600" CPU. The duration of the simulation is 9.5 hours for the FDTD method and 20 minutes for the worst-case adaptive model.

As an example, let us consider the analysis results obtained for the observation point (-0.72, -2.28, 1.43) m in case of the E1 HEMP disturbance. This point is located inside the "back" compartment of the vehicle (see Fig. 5).

Fig. 6 shows the waveform of the incident pulse and the response waveform calculated by different methods. The waveform of the projection of the field vector onto the basis vector is considered as the FDTD calculation result; here, the basis vector is the field vector at the instant of time when the field amplitude at the worst point (see Fig. 5) is maximal.

Fig. 7 shows the amplitude spectra of the waveforms displayed in Fig. 6. For the worst-case adaptive model, the f_{mx} value for the considered observation point is 74.6 MHz.

For the considered observation point, the use of the worst-case adaptive model reduces the overestimation of the peak amplitude of the response by a factor of 8.2 (from 4993 / 151.3 = 33.00 (V/m)/(V/m) to 612.6 / 151.3 = 4.049 (V/m)/(V/m), see Fig. 6), while maintaining the worst-case nature of the calculation results.

In case of the radar pulse, the use of the worst-case adaptive model does not lead to an underestimation of the response amplitude (see Figs. 8 and 9).

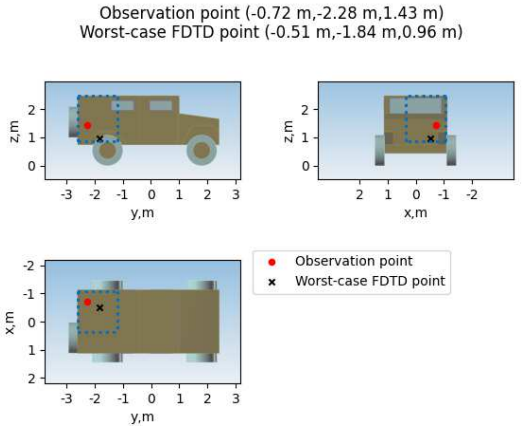

Fig. 5. Observation point (-0.72, -2.28, 1.43) m, its vicinity (blue dotted line), and the worst point obtained by worst-case FDTD model

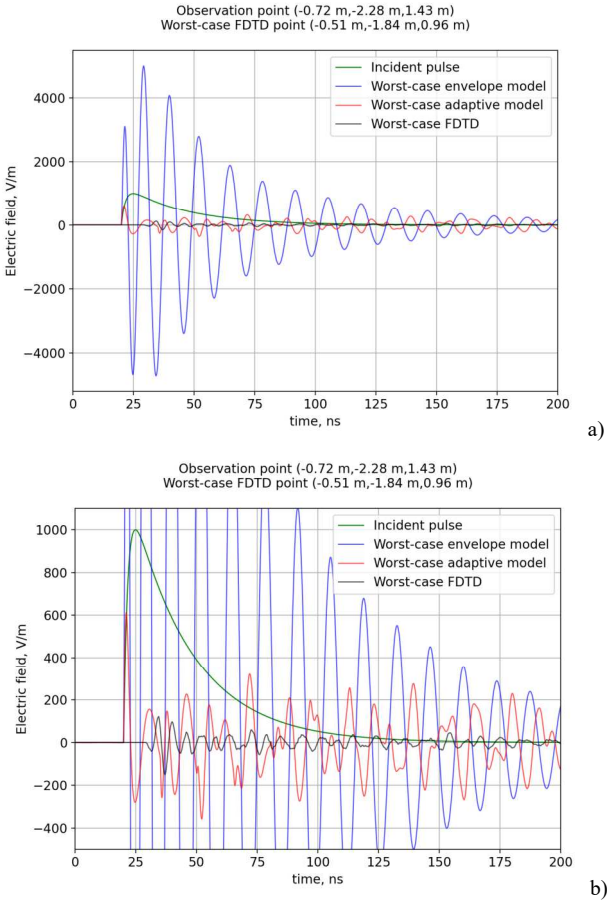

Fig. 6. Electric field waveforms of incident E1 HEMP pulse and response to this pulse: a), b) – different display scales

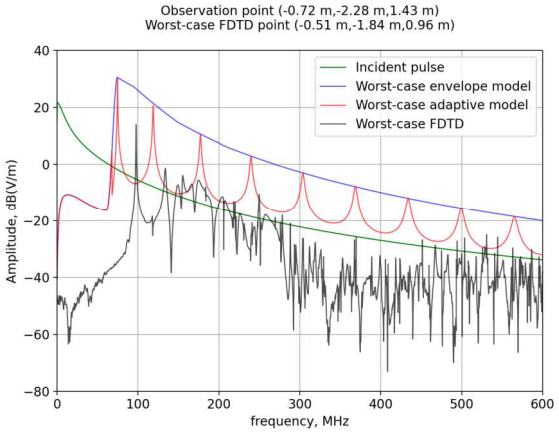

Fig. 7. Amplitude spectra of electric field for incident E1 HEMP pulse and for response to this pulse

Tables I and II are formed by processing analogous results obtained for all observation points. The average (over all considered observation points inside the compartments of the vehicle) overestimation of the peak amplitude of the response to the E1 HEMP disturbance is decreased by 13.2 dB (i.e., 4.6 times, see Table I) as a result of replacing the worst-case envelope model with the worst-case adaptive model; but the average overestimation of the amplitude of the response to the radar pulse has little change (see Table II), because the bandwidth of the radar pulse is less than the width of the corresponding peak in the AFC of the worst-case adaptive model. These data confirm the advantage of

the developed adaptive model over the traditional worst-case envelope model.

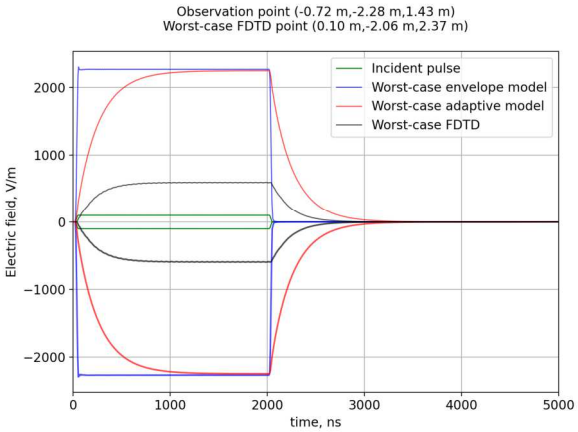

Fig. 8. Time-domain envelopes of electric field waveforms for incident radar pulse and for response to this pulse

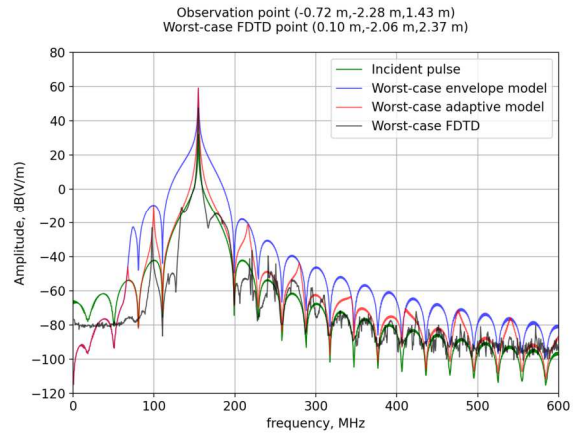

Fig. 9. Envelopes of amplitude spectra of electric field for incident radar pulse and for response to this pulse

TABLE I. OVERESTIMATION OF PEAK AMPLITUDE FOR RESPONSE TO E1 HEMP PULSE (STATISTICS FOR ALL OBSERVATION POINTS)

Worst-case model	**Overestimation of pulse amplitude**					
	Min		**Max**		**Average**	
	dB	V/m / V/m	dB	V/m / V/m	dB	V/m / V/m
Envelope	16.53	6.71	34.77	54.76	24.41	16.61
Adaptive	2.52	1.34	19.28	9.20	11.17	3.62

TABLE II. OVERESTIMATION OF PEAK AMPLITUDE FOR RESPONSE TO RADAR PULSE (STATISTICS FOR ALL OBSERVATION POINTS)

Worst-case model	**Overestimation of pulse amplitude**					
	Min		**Max**		**Average**	
	dB	V/m / V/m	dB	V/m / V/m	dB	V/m / V/m
Envelope	11.70	3.85	15.22	5.77	13.83	4.92
Adaptive	11.47	3.75	14.76	5.47	13.48	4.72

IV. CONCLUSION

The performed validation (see Section III.C) confirms the operability and usefulness of the proposed approach and the developed worst-case adaptive model in solving problems of analyzing and ensuring EMC and electromagnetic protection of electronic equipment. The proposed approach and the developed model are implemented in specialized software intended to design the protection of complex radio-electronic systems from powerful electromagnetic disturbances.

The use of worst-case adaptive models makes it possible to eliminate both the underestimation of the critical parameters (energy, power, peak amplitude) of the object's response to electromagnetic disturbance, which is typical for particular-case models, and the overestimation of these parameters, which is typical for worst-case envelope models (see Tables I and II). Therefore, worst-case adaptive models can be used instead of traditional worst-case envelope models when solving the problems of EMC and electromagnetic protection.

The developed model (see Section III.B) uses the simplified algorithm of semi-analytical optimization (see Section II); this makes it possible to increase the speed of calculations by a large factor as compared to the methods of computational electromagnetics (see Section III.C).

REFERENCES

[1] C. R. Paul, *Introduction to Electromagnetic Compatibility*, 2nd ed. Hoboken, NJ, USA: Wiley, 2006.

[2] H. W. Ott, *Electromagnetic Compatibility Engineering*, rev. ed. Hoboken, NJ, USA: Wiley, 2009.

[3] W. G. Duff, *Designing Electronic Systems for EMC*, Raleigh, NC, USA: SciTech Publishing, 2011.

[4] A. Mori, P. di Bartolomeo, M. Bandinelli et al. "Design-oriented EMC analysis of wiring systems," in *Proc. Int. Symp. "EMC Europe"*, 2020, pp. 1–6.

[5] S. Arianos, M. A. Francavilla, M. Righero et al. "Evaluation of the modeling of an EM illumination on an aircraft cable harness," *IEEE Trans. Electromagn. Compat.*, vol. 56, no. 4, pp. 844–853, Aug. 2014

[6] J. L. Bogdanor, R. A. Pearlman, and M. D. Siegel "Intrasystem electromagnetic compatibility analysis program. Volume I: User's manual engineering section," Mc.Donnel Douglas Aircraft Corp., St. Louis, MO, USA, Rep. RADC-TR-74-342, Dec. 1974.

[7] X. Dong, H. Weng, D. G. Beetner, and T. H. Hubing "Approximation of worst case crosstalk at high frequencies," *IEEE Trans. Electromagn. Compat.*, vol. 53, no. 1, pp. 202–208, Feb. 2011.

[8] Y. Y. Arlou, E. V. Sinkevich, S. V. Maly, and G. Y. Slepyan "Computationally-effective worst-case model of wire radiation in the frequency range 1 Hz – 40 GHz," in *Proc. Int. Symp. "EMC Europe"*, 2014, pp. 1293–1298.

[9] D. Tsyanenka, E. Sinkevich, and Y. Arlou "Wideband worst-case model of electromagnetic field shielding by metallic enclosure with apertures," in *Proc. Int. Symp. "EMC Europe"*, 2017, pp. 1–6.

[10] E. Yavolovskaya, S. Iosava, Z. Sukhiashvili et al. "A study of stochasticity effects of cable bundles in automotive EMC problems," in *Proc. Int. Symp. "EMC Europe"*, 2010, pp.197–202.

[11] L. Wang, W. J. Koh, and Y. H. Lee "Out-of-band gain prediction of blade antennas for EMC purpose," in *Proc. Asia-Pacific Symp. EMC*, 2012, pp. 589–592.

[12] V. Mordachev, E. Sinkevich, D. Tsyanenka et al. "EMC diagnostics of complex radio systems by the use of analytical and numerical worst-case models for spurious couplings between antennas," in *Proc. Int. Symp. "EMC Europe"*, 2016, pp. 608–613.

[13] R. A. Pearlman "Physical interpretation of the IEMCAP integrated EMI margin," in *Proc. IEEE Int. Symp. EMC*, 1978, pp. 310–315.

[14] *Electromagnetic Compatibility (EMC) – Part 5-9: Installation and Mitigation Guidelines – System-Level Susceptibility Assessments for HEMP and HPEM*, IEC/TS 61000-5-9, 2009-07.